
**This is a postprint of an article published in**
**El-Enshasy, H., Kleine, J., Rinas, U.**
**Agitation effects on morphology and protein productive fractions of filamentous and pelleted growth forms of recombinant Aspergillus niger**
**(2006) Process Biochemistry, 41 (10), pp. 2103-2112.**

# Agitation effects on morphology and protein productive fractions of filamentous and pelleted growth forms of recombinant *Aspergillus niger* §

**Hesham El-Enshasy[#], Joachim Kleine, and Ursula Rinas***

Biochemical Engineering Division, GBF German Research Center for Biotechnology, Mascheroder Weg 1, 38124 Braunschweig, Germany

§ This article is dedicated to Wolf-Dieter Deckwer on the occasion of his 65th anniversary.

Cite as:

El-Enshasy, H., Kleine, J. and Rinas, U. (2006) Agitation effects on morphology and protein productive fractions of filamentous and pelleted growth forms of recombinant *Aspergillus niger*. Process Biochem., 41, 2103-2112.

Running title: Protein production by *Aspergillus niger*

# Current address: Bioprocess Development Department, Mubarak City for Scientific Research, New Burg Al-Arab, Alexandria, Egypt

* Corresponding author: Tel: 0049-531-6181-126; Fax: 0049-531-6181-111, E-mail: URI@gbf.de

**Abstract:** Recombinant *Aspergillus niger* genetically engineered to produce glucose oxidase using the constitutive *gpdA* promoter and the glucoamylase signal sequence for secretion was grown in batch cultures at agitation speeds of 200 – 800 rpm covering the industrial relevant power input range of 0.1 – 5 W $kg^{-1}$. The growth morphology ranged from large pellets with an average diameter of 1500 μm at low power input up to micropellets embedded in a filamentous network at high power input. A correlation of agitation intensity with growth morphology and glucose oxidase production revealed an increase of the protein production capability with the change of the growth morphology from pelleted to filamentous growth forms. However, the exposure to higher shear stress with increasing power input also resulted in lower biomass yields as well as increased transient formation of polyol (xylitol) and higher final concentrations of oxalic acid. The highest specific production rates were found in young filamentous growth forms at high power input. Although intermediate agitation intensity leading to small pellets became more favorable during prolonged cultivation. An acridine orange staining procedure discriminating between RNA rich (red) and RNA poor regions (green) of the fungal biomass proved that active protein production is restricted to filamentous growth forms and the outer layer of fungal pellets. A correlation between the RNA rich fraction of the biomass determined by image analysis and the productivity is shown.

*Keywords:* recombinant *Aspergillus niger*, glucose oxidase, morphology, protein excretion, agitation

## 1. Introduction

The success of filamentous fungi for industrial production of biotechnological products is largely due to the metabolic versatility of this group of microorganisms. Filamentous fungi such as *Aspergillus niger* are well-known for their excellent protein excretion capabilities; yields of 20 grams per liter extracellular glucoamylase, a homologous starch-degrading enzyme used in the food industry, have been reported [1]. Efforts have been also undertaken to develop *Aspergillus niger* for the production of heterologous proteins including biopharmaceuticals. In general, *A. niger* is an excellent host for the production of fungal proteins but high concentrations of heterologous (non-fungal) products are notoriously difficult to obtain [2,3]. Though commercially interesting levels of recombinant bovine chymosin, an enzyme used for cheese manufacture, have already been reported in the early nineties [4,5], other proteins, for example, biopharmaceuticals such as interleukin-6 [3], tissue plasminogen activator [6], single-chain antibodies [7], and hepatitis B pseudoviral particles [8] are still just found in milligram per liter quantities in the culture medium. Unsatisfactory low yields are often caused by proteolytic degradation of the target protein [6,9], with improvements being obtained by modifying culture conditions [6,10,11] and developing strains with less proteases [12,13]. Moreover, the complex and not well understood impact of environmental conditions on fungal morphology and resulting effects on protein production and excretion imposes an additional handicap for a more widespread distribution of *Aspergillus* as a recombinant protein producer. However, bioprocessing strategies can greatly contribute to further improvements of recombinant fungal cultivation processes [14].

Filamentous fungi such as *A. niger* exhibit different growth morphologies in submerged culture varying from compact pelleted to filamentous growth forms which strongly affect the overall cell performance [15]. An important advantage of the pelleted morphology is the decrease in viscosity of the culture fluid, resulting in improved mixing and mass transfer properties. In addition, the pelleted growth form facilitates downstream processing by

simplifying solid-liquid separation procedures. The major disadvantages of pelleted growth forms are mass transfer limitations leading to significant concentration gradients of oxygen and other nutrients from the culture fluid to the inner pellet core [16-20]. These limitations can finally result in autolytic processes within the inner part of big fungal pellets [17-19,21].

The morphology of *Aspergillus*, filamentous growth forms and/or the shape and size of pelleted growth forms as well as the branching frequency, is influenced by many factors including specific strain properties [22] but also environmental factors such as spore numbers in the inoculum or type of inoculum [23-25], medium composition [23,26-28], dissolved oxygen concentration [29-31], pH [23,32], temperature [23,27], reactor type and scale [27,33], and power input [23,25, 26,28,29,33-36].

In particular, power input or agitation intensity has been identified as an important variable influencing the fungal morphology and productivity in recombinant *Aspergillus* protein production processes [25,28,37-39]. In general, increasing power input changes the growth morphology from pelleted to filamentous growth forms. With respect to protein production, there are conflicting results on the effect of agitation intensity. For example, power input greatly influenced morphology and extracellular hen egg white lysozyme production by recombinant *Aspergillus niger* with highest productivities obtained at intermediate agitation speed in batch culture [37]. On the other hand, production of an extracellular cutinase by recombinant *Aspergillus awamori* was found to be independent on the agitation intensity in fed-batch cultures [25]. Also, production of extracellular amyloglucosidase by recombinant *Aspergillus oryzae* was reported to be independent on power input variations in chemostat cultures at constant dilution rate [38]. During batch cultivation, however, production of extracellular amyloglucosidase increased with increasing agitation speed while agitation speed variations had no significant effect on protein production in fed-batch cultures [39].

In this work, we employed a recombinant strain of *Aspergillus niger* genetically engineered to produce glucose oxidase using the constitutive *gpdA* promoter and the glucoamylase signal

sequence for secretion [40]. This strain produces glucose oxidase during growth on glucose but also during growth on other carbon sources such as fructose or xylose [41]. Moreover, glucose oxidase is excreted to the culture medium although delayed to synthesis and incompletely due to retention in the cell wall and the inner pellet core [21,42]. Glucose oxidase synthesis and excretion are strongly influenced by culture conditions and morphology [21].

In this study, we analyzed in detail the impact of agitation intensity on growth morphology and on glucose oxidase synthesis and excretion. In addition, acridine orange staining and fluorescence microscopy was used to differentiate between productive (rich in RNA) and non-productive (poor in RNA) parts of the fungal biomass. Finally, a correlation between RNA rich biomass and productivity is shown.

## 2. Materials and methods

### *2.1 Strain*

The construction of recombinant *A. niger* NRRL-3 (GOD 3-18), carrying multiple copies of the *god* gene fused to the α-amylase signal sequence and controlled by the constitutive *gpdA*-promoter has been described before [40].

### *2.2 Culture conditions*

Inoculation was carried out by $1\times10^7$ spores $mL^{-1}$ obtained from a densely conidiating culture grown on CM agar medium for 48-72 h. CM-agar plates for sporulation were prepared as described previously [40]. The composition of the culture medium was as follows [g $L^{-1}$]: xylose, 80.0; $NaNO_3$, 3.0; $K_2HPO_4$, 1.0; $MgSO_4.7H_2O$, 0.5; KCl, 0.5; $FeSO_4.7H_2O$, 0.01 and yeast extract, 2.0. [41]. The pH of the medium was adjusted to pH 5.5 before autoclaving. Xylose was sterilized separately and added to the culture prior to inoculation.

Cultivations were carried out in a 5-L stirred tank bioreactor Biostat MD (B.Braun Diesel Biotech, GmbH) with a working volume of 3 L. The stirrer of the Biostat MD was equipped with three 6-bladded rushton turbine impellers ($d_i$=64 mm, $d_t$ =160 mm, $hd_t^{-1}$= 1.0; $d_id_t^{-1}$ = 0.4). The agitation was adjusted at 200 rpm for the first 5 hours of the cultivation and adjusted to the selected agitation speed for the rest of cultivation. Aeration was performed by filtered sterile air (0.75 L $min^{-1}$ during the first 5 hours of cultivation and 1.5 L $min^{-1}$ afterwards). The decreased agitation and aeration during the first hours of cultivation was performed to prevent spore flocculation and adhesion to the wall of the culture vessel. Cultivations were carried out at agitation speeds of 200, 500, and 800 rpm which roughly corresponds to an energy dissipation rate of 0.1, 2, and 5-8 W $kg^{-1}$ according to Cui et al. [43], respectively. The pH was controlled at pH 5.5 by the addition of 2.5 mol $L^{-1}$ NaOH. Foam was suppressed, when necessary, by the addition of antifoam reagent SP1 (Th. Goldschmidt AG, Essen, Germany). The digital control unit of the Biostat MD bioreactor, mass flow meter, balance of NaOH

solution, pumps and exhaust-gas analysis system were interfaced to a VME-bus microcomputer using UBICON (Universal Bio-Process Control System) software for data acquisition and processing. The concentrations of oxygen and carbon dioxide in the exhaust gas were determined by paramagnetic and infrared gas analysis systems, respectively (Maihak, Germany). Dissolved oxygen concentrations were analyzed by a polarographic electrode (Ingold, Mittler-Toledo, Switzerland).

*2.3 Analytical methods*

Sample preparation and analysis of cell dry mass (CDM), and endo- and exocellular GOD activities were carried out as described previously [40,42]. The quantitative determination of xylose, organic acids and xylitol were carried out by HPLC using an Aminex HXP-87H column (BioRad) for separation (T=25°C) and ultravilotet (UV) and refractive index detectors (Techlab, Germany) for detection. Sulfuric acid (5 mmol $L^{-1}$) was used as mobile phase (flow rate = 0.5 mL $min^{-1}$). Nitrate was determined using an ion-selective electrode model Orion 93-07 (reference electrode model Orion 90-02; both from Orion Research, Boston, USA). Ortho-phosphate ions in the cultivation broth were determined according to the method of Boltz [44].

*2.4 Carbon balance*

A simplified carbon balance was determined as described by Nowakowska-Waszczuk and Sokolowski [45].

$$X \cdot \sigma_X + Xyl \cdot \sigma_{Xyl} + Ox \cdot \sigma_{Ox} + dCO_2 \cdot \sigma_{CO_2} = S \cdot \sigma_S \qquad (1)$$

where $S$ is the mass of utilized sugar (xylose) and $X$, $Xyl$, $Ox$, and $dCO_2$ the masses of biomass, xylitol, oxalate and carbon dioxide produced, respectively. Their carbon content is denoted as $\sigma_S$, $\sigma_X$, $\sigma_{Xyl}$, $\sigma_{Ox}$, and $\sigma_{CO_2}$, respectively.

The elemental composition of the biomass was determined as $CH_{1.74}\ O_{0.711}\ N_{0.117}$ (performed in Analytische Laboratorien Co. Gummersbach, Germany) and the carbon content of the biomass was considered to be constant throughout the cultivation. The carbon present in yeast extract and extracellular glucose oxidase was neglected in this mass balance.

*2.5 Cell morphology studies, acridine orange staining, and productive biomass determination*

A sample taken from the bioreactor was directly mixed with 96% ethanol to stop nucleic acid turnover. Fixation was carried out on microscopic slides for 60 min at 80°C. The fixed samples were stained using acridine orange (400 μmol $L^{-1}$ acridine orange in 0.1 mol $L^{-1}$ Na-phosphate buffer, pH 7.0) according to the method described in Freudenberg et al. [46]. After 2 min, the dye solution was removed by washing with distilled water and the samples were allowed to dry again at room temperature. The green and red fluorescence was visualized using a fluorescence microscope (Leica DM LB, Germany) with a I-3 filter. A video camera (CCD-colored video camera CF 15/4 MCC, Kappa, Germany) was connected to the microscope via the image control unit MCU/C. Image analyzer software (Leica Q500 MC, Leica, Germany) was used for the morphological characterization. The diameter of each pellet or bioparticle as well as the productive (total minus inner green stained part) and unproductive fraction (green stained part) of the pellet were measured manually at six different positions to account for shape irregularities (by touching two opposite points using a mouse). The average from these measurements were taken as average diameter of each pellet or bioparticle as well as the productive and unproductive fraction of the pellet. The inner green strained part of the pellet which is rich in DNA (and poor in RNA) was considered as unproductive fraction with respect to protein synthesis. The outer layer of the pellet, which emitted red fluorescence was considered as the productive fraction of the pellet (rich in RNA). In all cases, the data shown are an average of randomly selected 100-120 particles.

## 3. Results and discussion

### *3.1 Agitation Effects on growth and glucose oxidase production*

Recombinant *A. niger* NRRL-3 (GOD 3-18) was grown in batch culture at different agitation speeds (200, 500, and 800 rpm). Except for agitation speed variations, all other process variables were kept constant to allow for the determination of the power input influence on the overall process performance. Moreover, the agitation speed was not changed throughout the cultivations, except for the first 5 h after inoculation where is was kept at 200 rpm in all cultivations to prevent spore flocculation and adhesion to the wall of the culture vessel.

#### *3.1.1 Cultivation at low power input (200 rpm)*

After 60 hours of cultivation the biomass reached around 30 g $L^{-1}$ and did not increase any further (Fig. 1A). Xylose, nitrate, and phosphate did not decline to growth limiting concentrations, however, the dissolved oxygen concentration in the bulk phase reached limiting concentrations 50 h after inoculation and remained low for the reminder of the cultivation (Fig. 1A). Total glucose oxidase activities reached around 300 μkat $L^{-1}$ (Fig. 1B). Glucose oxidase was first formed as a cell-bound enzyme and slowly released into the culture medium, after 100 h of cultivation half of the glucose oxidase formed was found as extracellular enzyme. Xylitol formation preceded oxalate formation, but was formed transiently (35 - 50 h of cultivation) and only minor amounts were detectable (maximum of 2.1 g $L^{-1}$). Oxalate reached 6.3 g $L^{-1}$ which represents 5.2% of xylose carbon supplied (Fig. 1C).

#### *3.1.2. Cultivation at medium power input (500 rpm)*

During the cultivation at medium power input less biomass was formed than at low speed agitation (Fig. 2A). The biomass formed did not surpass 25 g $L^{-1}$. Nitrate, phosphate, and the dissolved oxygen concentration in the bulk phase did not reach growth limiting

concentrations, but xylose was completely consumed after 85 h of cultivation. Total glucose oxidase activities reached more than 800 μkat $L^{-1}$ which is almost 3 times more than at low speed agitation (Fig. 2B). Again, glucose oxidase was first formed as a cell-bound enzyme and subsequently released to the culture medium. Compared to low speed agitation, is was released more rapidly and also to a greater portion (> 80% extracellular glucose oxidase). Cultivation at medium power input resulted in more xylose carbon being transformed to oxalate and carbon dioxide. Oxalate reached 26 g $L^{-1}$ which represents 22% of xylose carbon supplied (Fig. 2C). Moreover, 50% of the xylose carbon was transformed into carbon dioxide (Fig. 2C) compared to only 20% at low power input (Fig. 1C). Also, more xylitol was transiently formed reaching the highest level of 5.2 g $L^{-1}$ after 45 h of cultivation (Fig. 2C).

*3.1.3. Cultivation at high power input (800 rpm)*

Even less biomass was formed at high speed agitation where it reached only 15 g $L^{-1}$after 40 h of cultivation without any further increase (Fig. 3A). This corresponds to half of the biomass being formed at low speed agitation. Nitrate, phosphate, and the dissolved oxygen concentration in the bulk phase did not reach growth limiting concentrations. Also, xylose was not completely consumed at the end of the cultivation. Total glucose oxidase concentration increased rapidly to 600 μkat $L^{-1}$ during the first 30 h of cultivation and did not increase any further thereafter (Fig. 2B) in contrast to the cultivations at lower speed agitation where total glucose oxidase activities increased less rapidly in the beginning but continued to increase throughout the cultivation (Figs. 1B and 2B). Oxalate was formed at even higher concentrations reaching final levels of 45 g $L^{-1}$ while carbon dioxide formation decreased compared to medium power input cultivation (Fig. 3C). At the end, 37 and 30% of the xylose carbon was transformed into oxalate and carbon dioxide, respectively. Xylitol was also formed transiently and reached the highest level of 6.4 g $L^{-1}$ after 60 h of cultivation (Fig. 3C).

*3.2 Power input effects on morphology and protein production and excretion*

To exclusively analyze the power input effect on fungal morphology and protein production and excretion and exclude any additional influence of other variables (e.g. oxygen limiting conditions versus non-limiting conditions), only the first 40 hours of the cultivations were analyzed in more detail. During this time period substrate consumption was comparable and none of the substrates reached growth-limiting concentrations (Figs. 1A-3A). Moreover, the evolution of the fungal biomass as determined by cell dry mass measurements did not reveal significant differences (Fig. 4A). Growth rate approximations assuming exponential cell growth revealed specific growth rates of 0.08 – 0.09 $h^{-1}$ for all cultures. In contrast, the fungal morphology was significantly affected by power input variations (Fig. 4B). Fungal pellets formed at low speed agitation reached an average pellet diameter of 1500 μm, at intermediate 400 μm and at high speed agitation only 24 μm (Fig. 4B). Moreover, distinct pellets with a hairy hyphal layer developed in low speed agitated cultures while micropellets formed at high power input were closely embedded in a filamentous network (see also Fig. 6). Pellet formation was completed 15 h post-inoculation, from this time on pellets increased in size but not in numbers. Pellet breakup and hollow pellets were not observed in these cultures. The average pellet diameter increased with a constant rate of 39.49 and 13.39 μm $h^{-1}$ in 200 and 500 rpm agitated cultures, respectively. The number of pellets was 45 $\pm$ 5 and 250 $\pm$ 40 pellets $ml^{-1}$ in cultures grown at 200 and 500 rpm, respectively. Pellet numbers were not determined in the high speed agitated cultures as the majority of fungal biomass was in the filamentous growth form (see also Fig. 6). Also, the mycelial network formed during the early cultivation phase revealed fragmentation to smaller filamentous clumps with ongoing cultivation time (cf Fig. 6E vs Fig. 6F).

Glucose oxidase production and excretion was also strongly affected by power input variations (Fig. 5). An increase of the agitation speed increased the total amount of glucose oxidase produced within the first 40 h of cultivation from 220 μkat $L^{-1}$ at low power input to 650 μkat $L^{-1}$ at high power input corresponding to 15 and 40 μkat per gram cell dry mass, respectively (Fig. 5A). Moreover, the maximum specific glucose oxidase production rates also increased with increasing power input reaching 1.5 and 13 μkat per hour and gram cell dry mass at low and high speed agitation, respectively (Fig. 5B). In all cultures the highest specific production rates were obtained 20 hours post-inoculation and rapidly declined thereafter. The elevated production of glucose oxidase with higher power input was also reflected in higher absolute extracellular glucose oxidase activities (Fig. 5C), however, the percentage of glucose oxidase released into the culture medium was not significantly affected by power input variations within this time period (Fig. 5D). During prolonged cultivation, however, the portion of glucose oxidase found in the culture medium increased with increasing power input and the corresponding change from the pelleted to the filamentous growth morphology (Figs. 1B-3B). These results are in accordance with previously reported findings that the release of the majority of the enzyme into the culture medium is delayed due to retention in the cell wall and pellet interior [42].

For the analysis of the productive part of the fungal biomass, an acridine orange staining technique was employed. Acridine orange intercalates with single- and double-stranded nucleic acids giving rise to red or green fluorescence when bound to RNA or DNA, respectively. As active protein production depends on the presence of single-stranded RNA, acridine orange staining can be used to discriminate between those parts of the fungal biomass which are rich in single-stranded RNA and, thus, potentially active with respect to protein synthesis and those parts which are poor in single-stranded RNA and where protein synthesis can not take place. Examples are shown in Figures 6 and 7, red fluorescence is exclusively

found at the outer hairy layer of the fungal pellet proving that only this part of the fungal biomass is rich in single stranded nucleic acids, namely mRNA, thus giving clear evidence that active protein production is restricted to the filamentous growth forms or the outer hairy layer of the fungal pellets. The pellet interior emits green and yellow fluorescence clearly proving that active protein production can not occur, or only in marginal amounts, within the inner part of fungal pellets. Moreover, these data also show that the red fluorescence in the hairy outer layer decreases with the cultivation time (Fig. 7) in accordance with the observed decline of the specific glucose oxidase production rates 20 h post-inoculation (Fig. 5B).

For determination of the productive fraction of the biomass, only those parts emitting red fluorescence were considered for quantification (Fig. 8A). The analysis of the culture grown at low speed agitation revealed that this part of the biomass rapidly decreased with culture time and increasing pellet size (Fig. 8B). From 40 hours post-inoculation onwards only 25% of the fungal biomass could be considered as potentially active with respect to protein synthesis. A comparative analysis of glucose oxidase production in the culture grown at low speed agitation and in the culture grown at high power input based on the estimation of the productive fraction of the biomass revealed comparable specific glucose oxidase acivities and production rates (Fig. 9). Thus, the lower overall productivities of big fungal pellets are a result of the lower fraction of productive biomass most likely caused by the reduced availability of nutrients in the inner pellet parts. This hypothesis is in agreement with model-based predictions that during rapid growth with unlimited supply of nutrients and oxygen in the bulk phase only the outer layer of the pellet with a thickness of approx. 50-100 μm has unlimited access to oxygen and other nutrients [19]. Moreover, microprobe measurements of oxygen profiles in fungal pellets corroborate the limited availability of oxygen in the core pellet region [17,20].

## 4. Conclusions

The growth morphology and protein production of *A. niger* is strongly influenced by power input variations. With increasing power input the growth morphology changes from pelleted to filamentous growth forms concomitant to an increase of the protein production capability. However, increasing power input also exposes the fungus to higher shear stress resulting in lower biomass yields and increased respiration and acid formation. The highest production rates are found in young more filamentous growth forms. However, intermediate power input leading to small pellets becomes more favorable during prolonged cultivation. Active protein production is restricted to filamentous growth forms and the outer layer of fungal pellets.

*Acknowledgments* – H. El-Enshasy wishes to thank the DAAD, Germany for financial support. We gratefully acknowledge critical reading of the manuscript by Xin Lu. Part of this study was carried out in the framework of the Sonderforschungsbereich 578 (Project B1/B4).

**References**


[1] Finkelstein DB. Improvement of enzyme production in *Aspergillus*. Antonie van Leeuwenhoek 1987;53:349-352.

[2] Archer DB, Peberdy JF. The molecular biology of secreted enzyme production by fungi. Crit Rev Biotechnol 1997;17:273-306.

[3] Punt PJ, van Biezen N, Conesa A, Albers A, Mangnus J, van den Hondel CAMJJ. Filamentous fungi as cell factories for heterologous protein production. Trends Biotechnol 2002;20:200-206.

[4] Ward M, Wilson LJ, Kodama KH, Rey MW, Berka RM. Improved production of chymosin in *Aspergillus* by expression as a glucoamylase-chymosin fusion. Bio/Technology 1990;8:435-440.

[5] Dunn-Coleman NS, Bloebaum P, Berka RM, Bodie E, Robinson N, Armstrong G, Ward M, Przetak M, Carter GL, LaCost R, Wilson LJ, Kodama KH, Baliu EF, Bower B, Lamsa M, Heinsohn H. Commercial levels of chymosin production by *Aspergillus*. Bio/Technology 1991;9:976-981.

[6] Wiebe MG, Karandikar A, Robson GD, Trinci APJ, Flores Candia J-L, Trappe S, Wallis G, Rinas U, Derkx PMF, Madrid SM, Sisniega H, Faus I, Montijn R, van den Hondel CAMJJ, Punt PJ. Production of tissue plasminogen activator (t-PA) in *Aspergillus niger*. Biotechnol Bioeng 2001;76:164-174.

[7] Joosten V, Lokman C, van den Hondel CAMJJ, Punt PJ. The production of antibody fragments and antibody fusion proteins by yeasts and filamentous fungi. Microb Cell Fact 2003;2:1.

[8] Plüddemann A, van Zyl WH. Evaluation of *Aspergillus niger* as host for virus-like particle production, using the hepatitis B surface antigen as a model. Curr Genet 2003;43:439-446.

[9] Archer DB, MacKenzie DA, Jeenes DJ, Roberts IN. Proteolytic degradation of heterologous proteins expressed in *Aspergillus niger*. Biotechnol Lett 1992;14:357-362.

[10] Xu J, Wang L, Ridgway D, Gu T, Moo-Young M. Increased heterologous protein production in *Aspergillus niger* fermentation through extracellular proteases inhibition by pelleted growth. Biotechnol Prog 2000;16:222-227.

[11] O'Donnell D, Wang L, Xu J, Ridgway D, Gu T, Moo-Young M. Enhanced heterologous protein production in *Aspergillus niger* through pH control of extracellular protease activity. Biochem Eng J 2001;8:187-193.

[12] van den Hombergh JPTW, Sollewijn Gelpke MD, van de Vondervoort PJI, Buxton FP, Visser J. Disruption of three acid proteases in *Aspergillus niger*: effects on protease spectrum, intracellular proteolysis, and degradation of target proteins. Eur J Biochem 1997;247:605-613.

[13] van den Hombergh JPTW, van de Vondervoort PJI, Fraissinet-Tachet L, Visser J. *Aspergillus* as a host for heterologous protein production: the problem of proteases. Trends Biotechnol 1997;15:256-263.

[14] Wang L, Ridgway D, Gu T, Moo-Young M. Bioprocessing strategies to improve heterologous protein production in filamentous fungal fermentations. Biotechnol Adv 2005;23:115-129.

[15] Grimm LH, Kelly S, Krull R, Hempel DC. Morphology and productivity of filamentous fungi. Appl Microbiol Biotechnol 2005;69:375-384.

[16] Kobayashi T, van Dedem G, Moo-Young M. 1973. Oxygen transfer into mycelial pellets. Biotechnol Bioeng 15:27-45.

[17] Wittler R, Baumgartl H, Lübbers DW, Schügerl K. Investigations of oxygen transfer into *Penicillium chrysogenum* pellets by microprobe measurements. Biotechnol Bioeng 1986;28:1024-1036.
[18] Cronenberg CCH, Ottengraf SPP, van Den Heuvel JC, Pottel F, Sziele D, Schügerl K, Bellgardt KH. Influence of age and structure of *Pencillium chrysogenum* pellets on the internal concentration profiles. Bioprocess Eng 1994;10:209-216.
[19] Rinas U, El-Enshasy H, Emmler M, Hille A, Hempel DC, Horn H. Model-based prediction of substrate conversion and protein synthesis and excretion in recombinant *Aspergillus niger* biopellets. Chem Eng Sci 2005;60:2729-2739.
[20] Hille A, Neu TR, Hempel DC, Horn H. Oxygen profiles and biomass distribution in biopellets of *Aspergillus niger*. Biotechnol Bioeng 2005;92:614-623.
[21] El-Enshasy H, Hellmuth K, Rinas U. Fungal morphology in submerged cultures and its relation to glucose oxidase excretion by recombinant *Aspergillus niger*. Appl Biochem Biotechnol 1999;81:1-11.
[22] Bocking SP, Wiebe MG, Robson GD,HK, Christiansen LH, Trinci APJ. Effect of branch frequency in *Aspergillus oryzae* on protein secretion and culture viscosity. Biotechnol Bioeng 1999;65:638-648.
[23] Schügerl K, Gerlach SR, Siedenberg D. 1998. Influence of the process parameters on the morphology and enzyme production of *Aspergilli*. Adv Biochem Eng Biotechnol 60:195-266.
[24] Papagianni M, Moo-Young M. Protease secretion in glucoamylase producer *Aspergillus niger* cultures: fungal morphology and inoculum effects. Process Biochem 2002;37:1271-1278.
[25] Johansen CL, Coolen L, Hunik JH. Influence of morphology on product formation in *Aspergillus awamori* during submerged fermentations. Biotechnol Prog 1998;14:233-240.
[26] Siedenberg D, Gerlach SR, Weigel B, Schügerl K, Giuseppin MLF, Hunik J. Production of xylanase by *Aspergillus awamori* on synthetic medium in stirred tank and airlift tower loop reactors: the influence of stirrer speed and phosphate concentration. J Biotechnol 1997;56:103-114.
[27] Gerlach SR, Siedenberg D, Gerlach D, Schügerl K, Giuseppin MLF, Hunik J. Influence of reactor systems on the morphology of *Aspergillus awamori*. Application of neural network and cluster analysis for characterization of fungal morphology. Process Biochem 1998;33:601-615.
[28] Wang L, Ridgway D, Gu T, Moo-Young M. Effects of process parameters on heterologous protein production in *Aspergillus niger* fermentation. J Chem Technol Biotechnol 2003;78:1259-1266.
[29] Cui YQ, van der Lans RGJM, Luyben KCAM. Effects of dissolved oxygen tension and mechanical forces on fungal morphology in submerged fermentation. Biotechnol Bioeng 1998;57:409-414.
[30] Wongwicharn A, McNeil B, Harvey LM. Effect of oxygen enrichment on morphology, growth, and heterologous protein production in chemostat cultures of *Aspergillus niger* B1-D. Biotechnol Bioeng 1999;65:416-424.
[31] Bai Z, Harvey LM, White S, McNeil B. Effects of oxidative stress on production of heterologous and native protein, and culture morphology in batch and chemostat cultures of *Aspergillus niger* (B1-D). Enzyme Microb Technol 2004;34:10-21.
[32] Carlsen M, Spohr AB, Nielsen J, Villadsen J. 1996. Morphology and physiology of an α-amylase producing strain of *Aspergillus oryzae* during batch cultivations. Biotechnol Bioeng 49:266-276.

[33] Cui YQ, van der Lans RGJM, Giuseppin MLF, Luyben KCAM. Influence of fermentation conditions and scale on the submerged fermentation of *Aspergillus awamori*. Enzyme Microb Technol 1998;23:157-167.
[34] Mitard A, Riba JP. Morphology and growth of *Aspergillus niger* ATCC 26036 cultivated at several shear rates. Biotechnol Bioeng 1988;32:835-840.
[35] Fujita M, Iwahori K, Tatsuta S, Yamakawa K. Analysis of pellet formation of *Aspergillus niger* based on shear stress. J Ferment Bioeng 1994;78:368-373.
[36] Cui YQ, van der Lans RGJM, Luyben KCAM. Effect of agitation intensities on fungal morphology of submerged fermentation. Biotechnol Bioeng 1997;55:715-726.
[37] Wongwicharn A, Harvey LM, McNeil B. Secretion of heterologous and native proteins, growth and morphology in batch cultures of *Aspergillus niger* B1-D at varying agitation rates. J Chem Technol Biotechnol 1999;74:821-828.
[38] Amanullah A, Blair R, Nienow AW, Thomas CR. Effects of agitation intensity on mycelial morphology and protein production in chemostat cultures of recombinant *Aspergillus oryzae*. Biotechnol Bioeng 1999;62:434-446.
[39] Amanullah A, Christensen LH, Hansen K, Nienow AW, Thomas CR. Dependence of morphology on agitation in fed-batch cultures of *Aspergillus oryzae* and its implications for recombinant protein production. Biotechnol Bioeng 2002;77:815-826.
[40] Hellmuth K, Pluschkell S, Jung J-K, Ruttkowski E, Rinas U. Optimization of glucose oxidase production by *Aspergillus niger* using genetic- and process-engineering techniques. Appl Microbiol Biotechnol 1995;43:978-984.
[41] El-Enshasy H, Hellmuth K, Rinas U. *GpdA*-promoter controlled production of glucose oxidase by recombinant *Aspergillus niger* using nonglucose carbon sources. Appl Biochem Biotechnol 2001;90:57-66.
[42] Pluschkell S, Hellmuth K, Rinas U. Kinetics of glucose oxidase excretion by recombinant *Aspergillus niger*. Biotechnol Bioeng 1996;51:215-220.
[43] Cui YQ, van der Lans RGJM, Luyben, KCAM. Local power uptake in gas-liquid systems with single and multiple rushton turbines. Chem Eng Sci 1996;51:2631-2636.
[44] Boltz DF. *In* Analytical chemistry of phosphate compounds Vol. II, Halmann, H. (Ed.) 1st edition, Wiley-Interscience, New York, 1972, pp. 31.
[45] Nowakowska-Waszczuk A, Sokolowski A. Application of carbon balance to submerged citric acid production by *Aspergillus niger*. Appl Microbiol Biotechnol 1987;26:363-364.
[46] Freudenberg S, Fasold K-I, Müller SR, Siedenberg D, Kretzmer G, Schügerl K, Giuseppin M. Fluorescence microscopic investigation of *Aspergillus awamori* growing on synthetic and complex media and producing xylanase. J Biotechnol 1996;46:265-273.

## Captions to Figures

**Figure 1.** Performance of recombinant *A. niger* NRRL-3 (GOD3-18) during cultivation at 200 rpm. The time course data of **(A)** cell dry mass (■), and the xylose (●), phosphate (▼), nitrate (▽) and dissolved oxygen concentrations (——), **(B)** the endo- (▲) and exocellular (△) and the total volumetric GOD activities (◆), and **(C)** the carbon balance represented as carbon content of xylose (gray), transformed to biomass (black), xylitol (sketches), oxalate (crossed sketches), and carbon dioxide (white) is shown.

**Figure 2.** Performance of recombinant *A. niger* NRRL-3 (GOD3-18) during cultivation at 500 rpm. The time course data of **(A)** cell dry mass (■), and the xylose (●), phosphate (▼), nitrate (▽) and dissolved oxygen concentrations (——), **(B)** the endo- (▲) and exocellular (△) and the total volumetric GOD activities (◆), and **(C)** the carbon balance represented as carbon content of xylose (gray), transformed to biomass (black), xylitol (sketches), oxalate (crossed sketches), and carbon dioxide (white) is shown.

**Figure 3.** Performance of recombinant *A. niger* NRRL-3 (GOD3-18) during cultivation at 800 rpm. The time course data of **(A)** cell dry mass (■), and the xylose (●), phosphate (▼), nitrate (▽) and dissolved oxygen concentrations (——), **(B)** the endo- (▲) and exocellular (△) and the total volumetric GOD activities (◆), and **(C)** the carbon balance represented as carbon content of xylose (gray), transformed to biomass (black), xylitol (sketches), oxalate (crossed sketches), and carbon dioxide (white) is shown.

**Figure 4.** Power input effects on **(A)** cell growth and **(B)** fungal morphology during growth at agitiation speeds of 200 (■), 500 (●), and 800 rpm (◆). Open and closed symbols correspond to data from different cultivations. The length of the bars in **(B)** represent the pellet size distribution.

**Figure 5.** Power input effects on glucose oxidase production and excretion. Time course data of **(A)** total glucose oxidase activities, **(B)** specific glucose oxidase production rates, and **(C)** absolute and **(D)** relative exocellular glucose oxidase activities during growth at agitiation speeds of 200 (■), 500 (●), and 800 rpm (◆). Open and closed symbols correspond to data from different cultivations.

**Figure 6.** Acridine-orange staining of fungal pellets for productive biomass determination. **(A, B)**, **(C, D)**, and **(E, F)** are from samples grown at the agitation speed of 200, 500, and 800 rpm, respectively. Fluorescent images of fungal biomass were taken **(A, C, E)** 19 h and **(B, D, F)** 25 h post-inoculation. The bar corresponds to 300 μm **(A, B, C, D, F)** and 75 μm **(E).**

**Figure 7.** Close-up of the apical tip region of acridine-orange stained pellets taken from the culture grown at 200 rpm. **(A)** Apical tip region after 15 h (bar = 75 μm), **(B)** 19 h (bar = 47.5 μm), **(C)** 23 h (bar = 37.5 μm), and **(D)** 50 h (bar = 75 μm) of cultivation.

**Figure 8.** Determination of the productive biomass based on the quantification of the RNA rich region of the fungal biomass. **(A)** Schematic and **(B)** productive biomass determination during cultivation at low speed agitation (200 rpm) considering only the red fluorescent part of the biomass.

**Figure 9.** Comparative analysis of **(A)** total specific glucose oxidase activities and **(B)** specific glucose oxidase production rates in cultures grown at agitation speeds of 200 (■) and 800 rpm (◆) considering the total (closed) and the productive part of the biomass (open symbols).

El-Enshasy et al., Figure 1

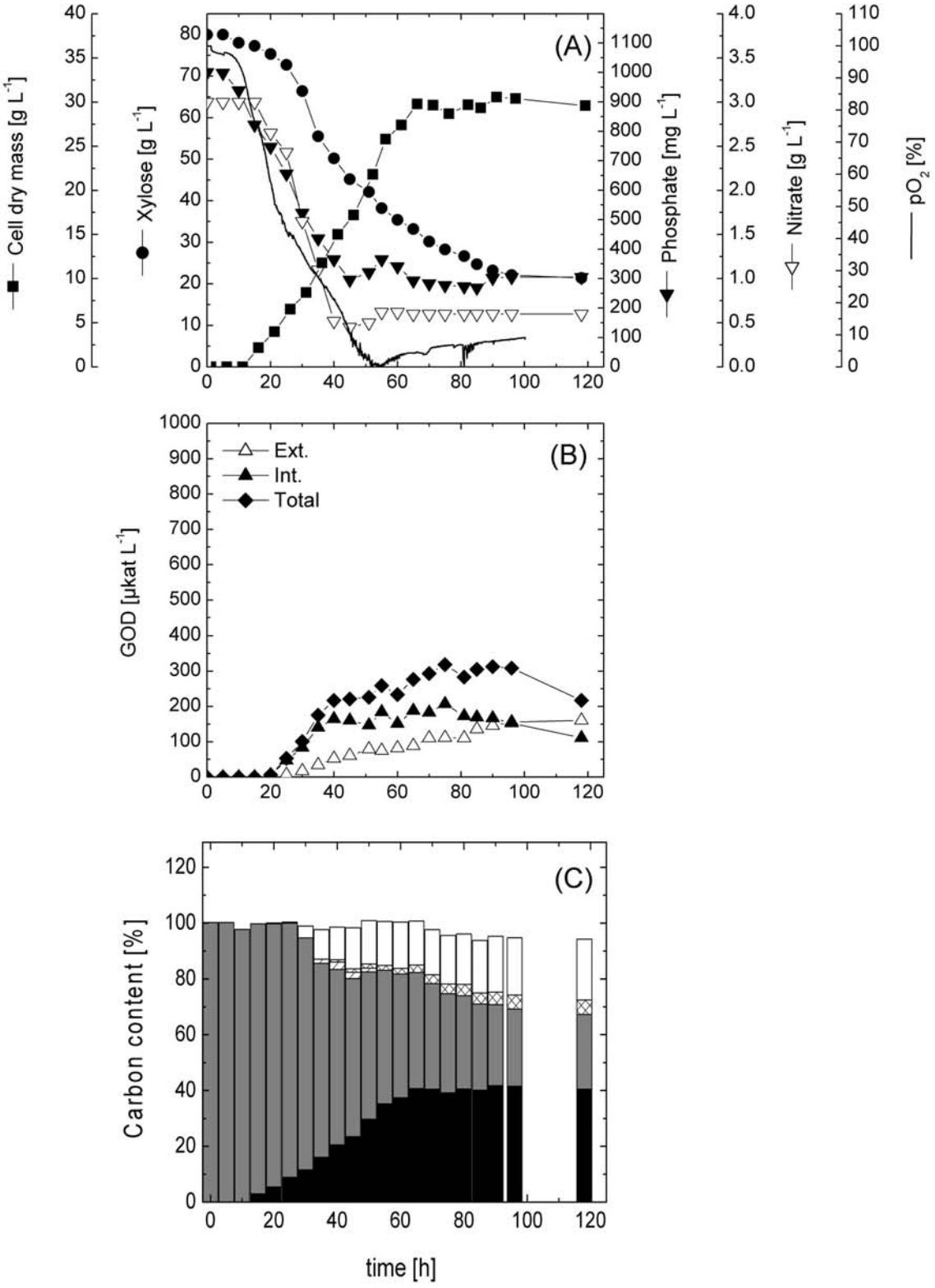

El-Enshasy et al., Figure 2

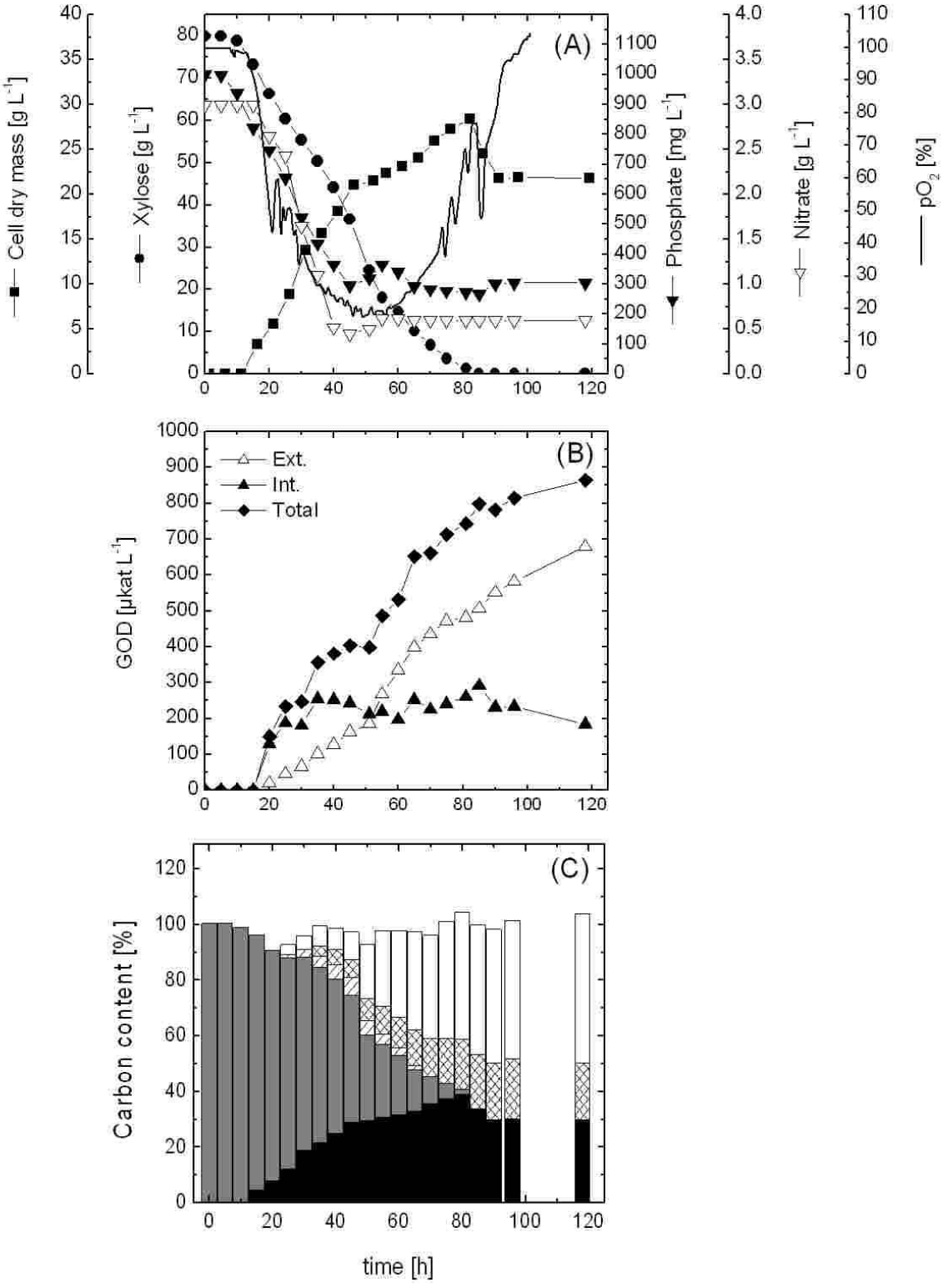

El-Enshasy et al., Figure 3

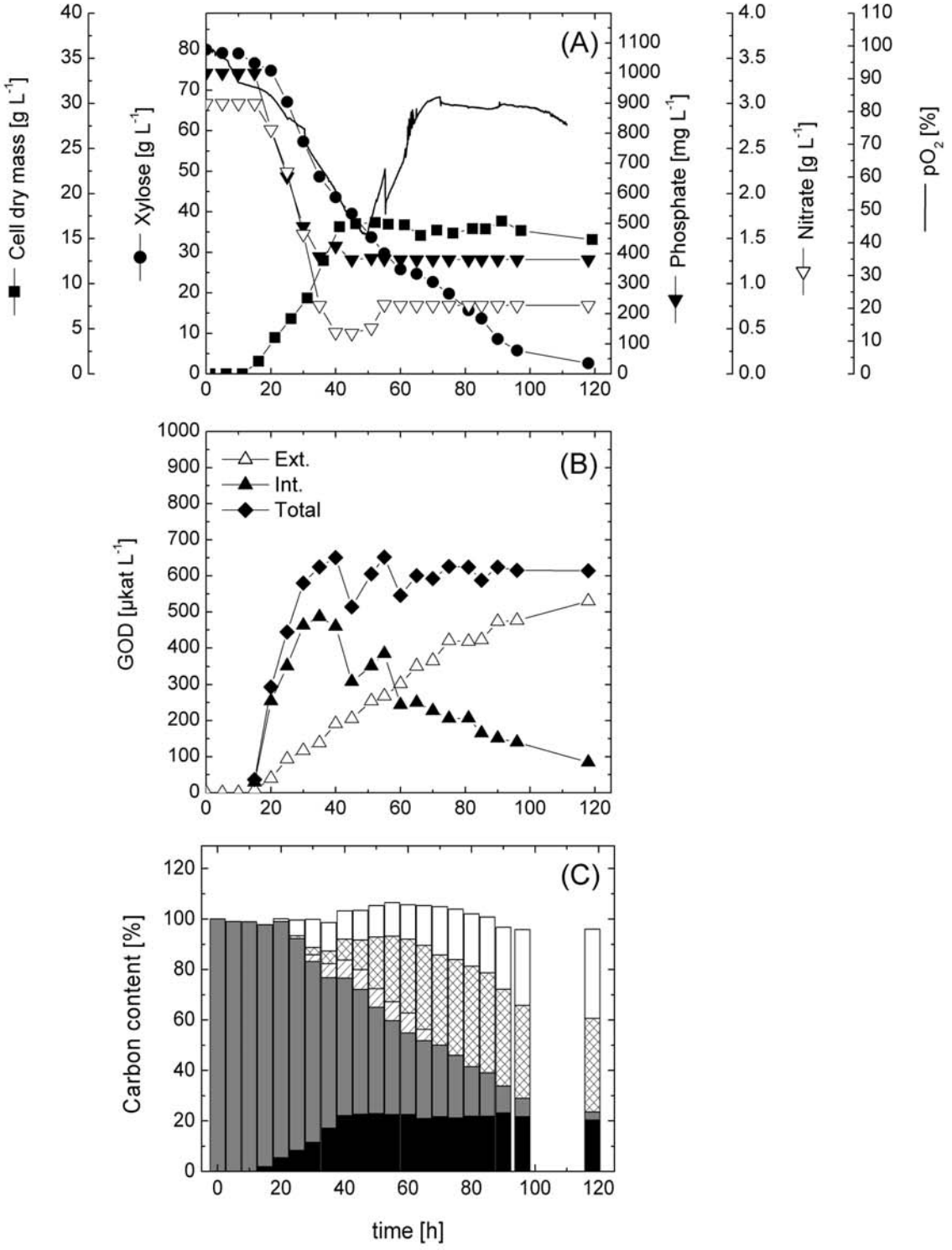

El-Enshasy et al., Figure 4

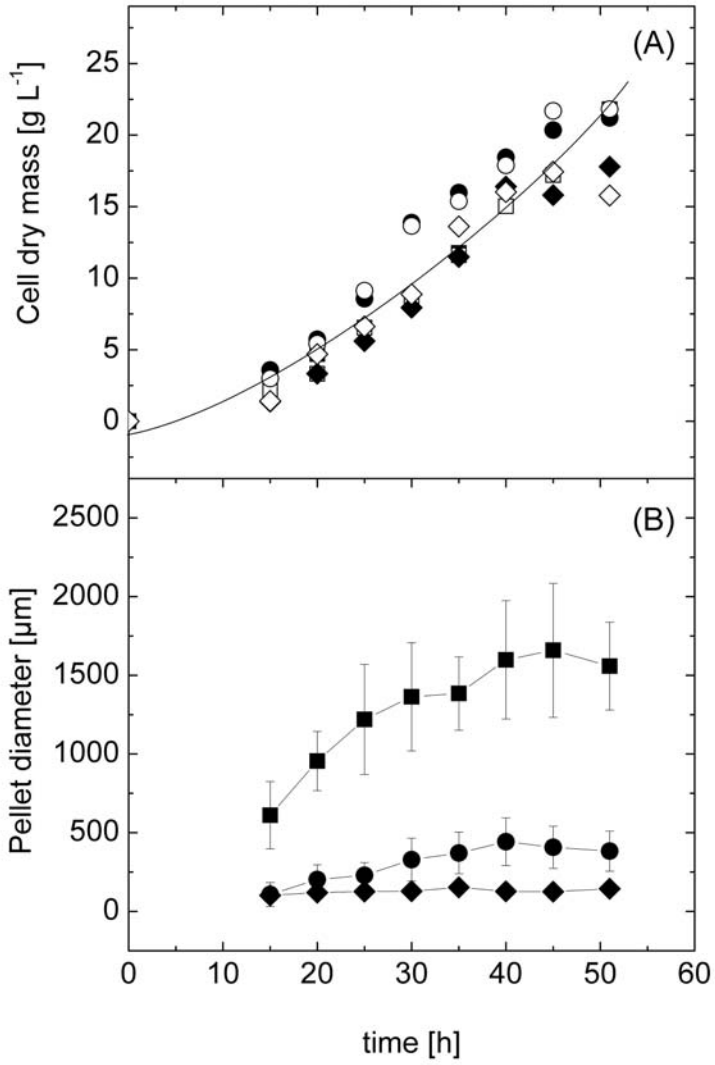

El-Enshasy et al., Figure 5

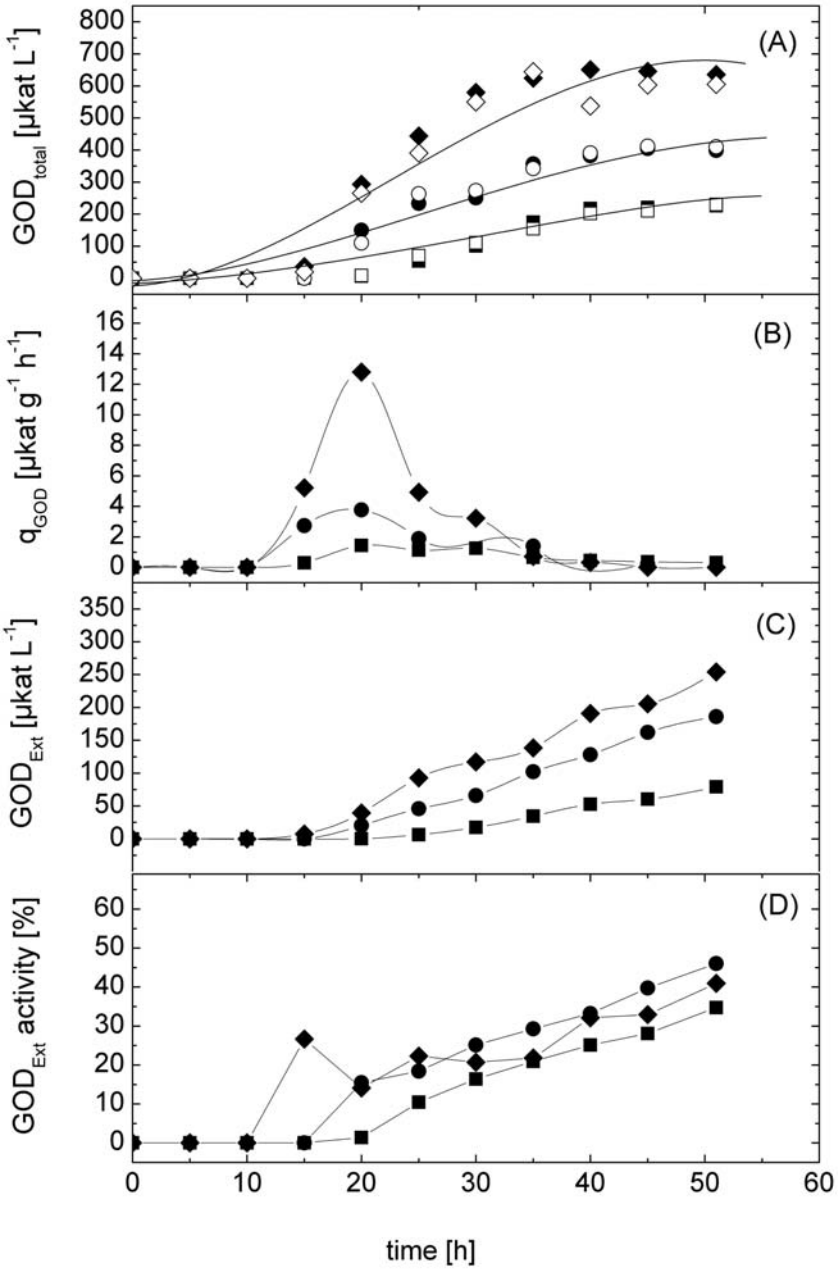

El-Enshasy et al., Figure 6

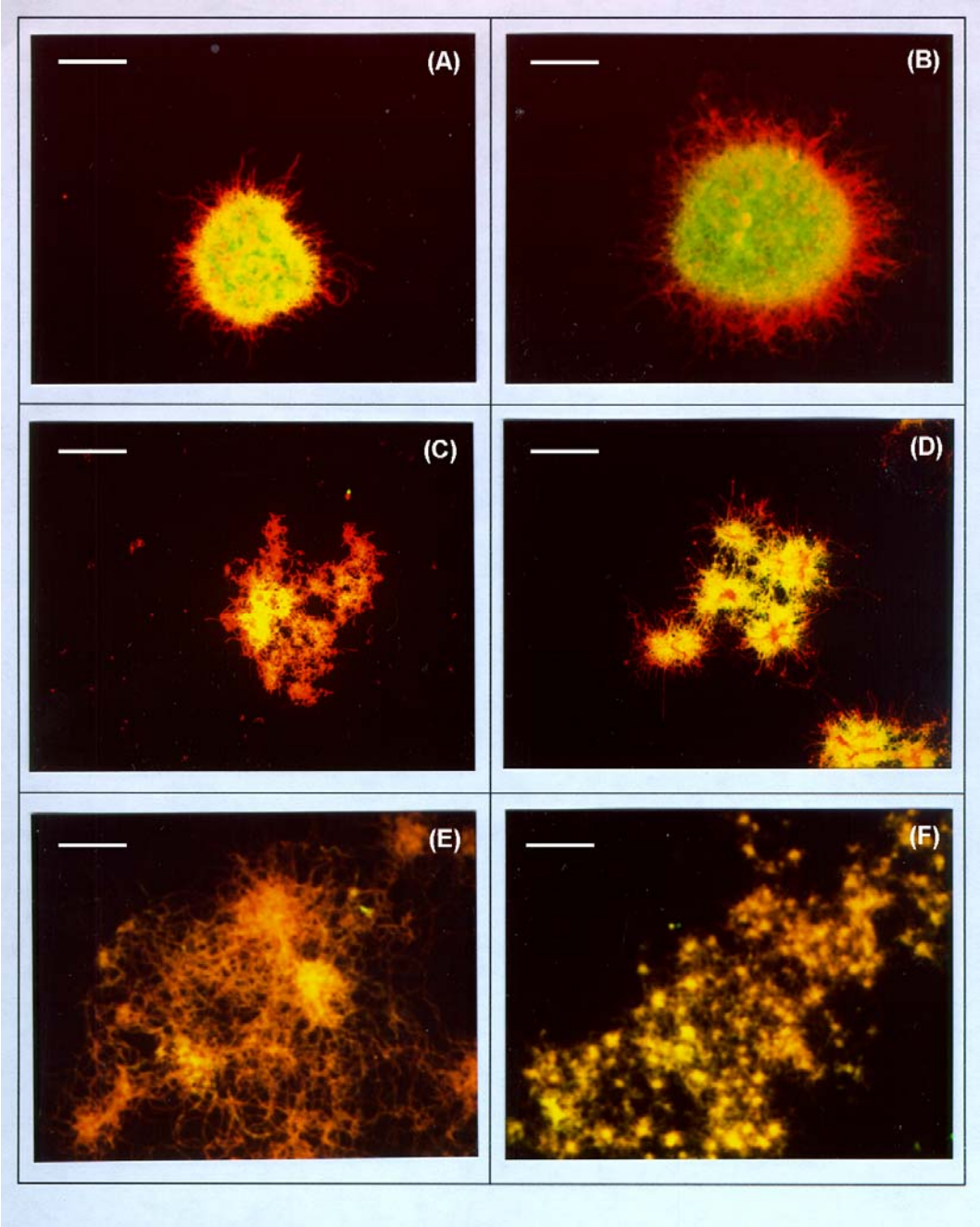

El-Enshasy et al., Figure 7

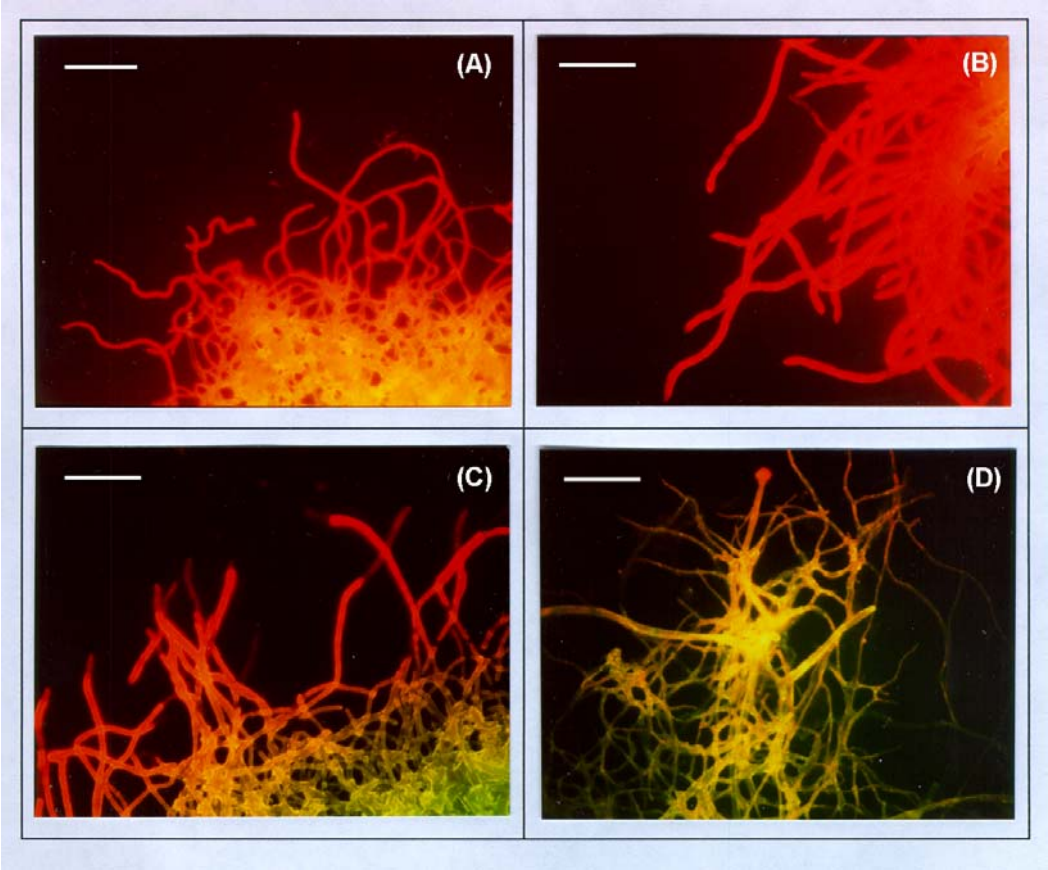

El-Enshasy et al., Figure 8

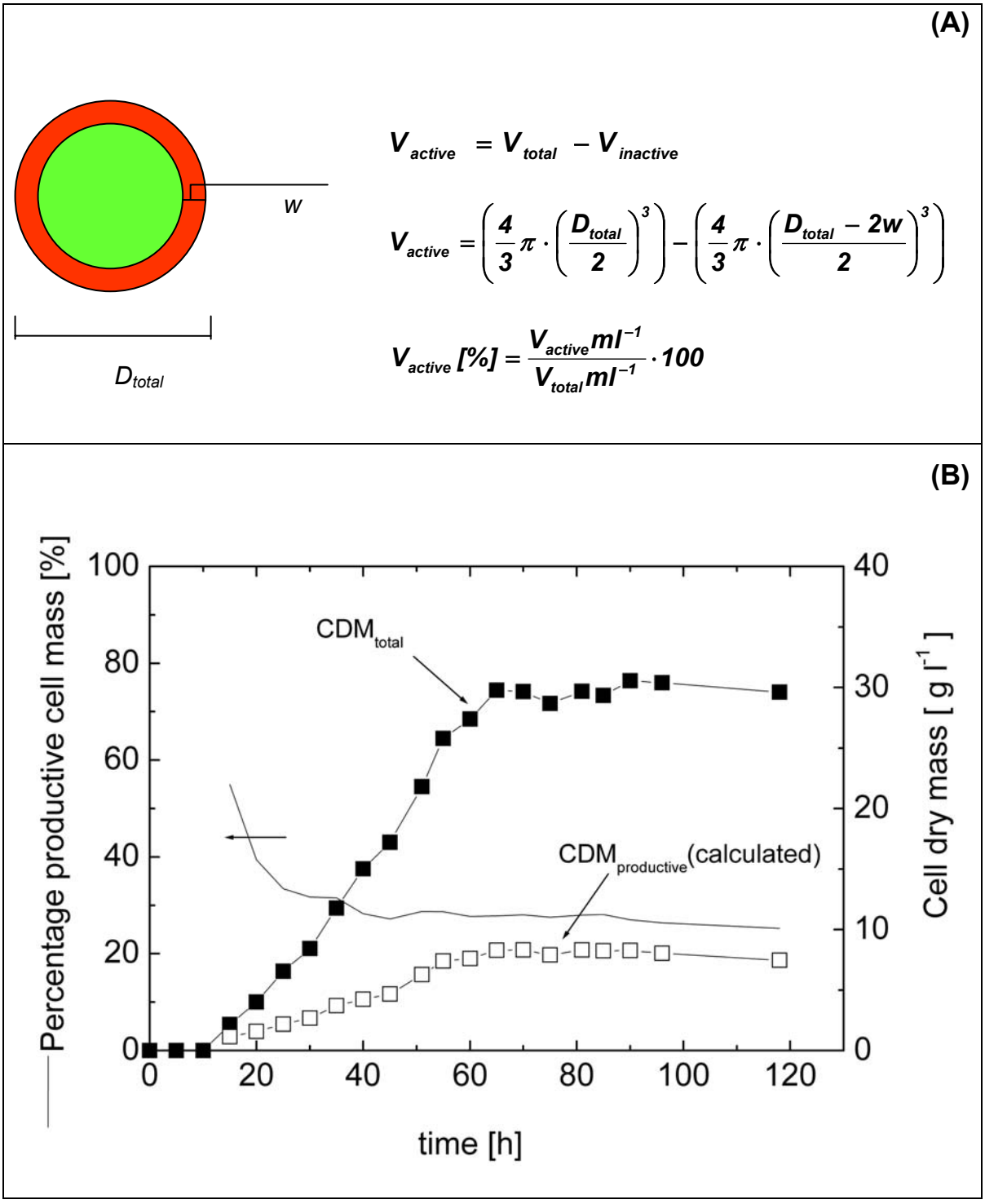

El-Enshasy et al., Figure 9